

Video Article

Investigating von Willebrand Factor Pathophysiology Using a Flow Chamber Model of von Willebrand Factor-platelet String Formation

Alison Michels¹, Laura L. Swystun¹, Jeffrey Mewburn², Silvia Alb  nez¹, David Lillicrap¹

¹Department of Pathology and Molecular Medicine, Queen's University

²Department of Medicine, Queen's University

Correspondence to: David Lillicrap at david.lillicrap@queensu.ca

URL: <https://www.jove.com/video/55917>

DOI: [doi:10.3791/55917](https://doi.org/10.3791/55917)

Keywords: Medicine, Issue 126, von Willebrand factor, platelets, endothelial cells, flow chamber, histones, Weibel-Palade bodies, shear stress, thrombosis.

Date Published: 8/14/2017

Citation: Michels, A., Swystun, L.L., Mewburn, J., Alb  nez, S., Lillicrap, D. Investigating von Willebrand Factor Pathophysiology Using a Flow Chamber Model of von Willebrand Factor-platelet String Formation. *J. Vis. Exp.* (126), e55917, doi:10.3791/55917 (2017).

Abstract

Von Willebrand factor (VWF) is a multimeric glycoprotein coagulation factor that mediates platelet adhesion and aggregation at sites of endothelial damage and that carries factor VIII in the circulation. VWF is synthesized by endothelial cells and is either released constitutively into the plasma or is stored in specialized organelles, called Weibel-Palade bodies (WPBs), for on-demand release in response to hemostatic challenge. Procoagulant and proinflammatory stimuli can rapidly induce WPB exocytosis and VWF release. The majority of VWF released by endothelial cells circulates in the plasma; however, a proportion of VWF is anchored to the endothelial cell surface. Under conditions of physiological shear, endothelial-anchored VWF can bind to platelets, forming a VWF-platelet string that may represent the nidus of thrombus formation. A flow chamber system can be used to visually observe the release of VWF from endothelial cells and the subsequent platelet capture in a manner that is reproducible and relevant to the pathophysiology of VWF-mediated thrombus formation. Using this methodology, endothelial cells are cultured in a flow chamber and are subsequently stimulated with secretagogues to induce WPB exocytosis. Washed platelets are then perfused over the activated endothelium. The platelets are activated and subsequently bind to elongated VWF strings in the direction of fluid flow. Using extracellular histones as a procoagulant and proinflammatory stimulus, we observed increased VWF-platelet string formation on histone-treated endothelial cells compared to untreated endothelial cells. This protocol describes a quantitative, visual, and real-time assessment of the activation of VWF-platelet interactions in models of thrombosis and hemostasis.

Video Link

The video component of this article can be found at <https://www.jove.com/video/55917/>

Introduction

Thrombosis is a leading cause of mortality worldwide¹ and can develop in response to dysregulated platelet activation and thrombin generation in both veins and arteries. Plasma levels of VWF are a key regulator of blood coagulation, whereby low levels (<50%) result in the bleeding disorder known as von Willebrand disease (VWD)² and high levels (>150%) are associated with an increased risk of venous³ and arterial⁴ thrombosis.

VWF is a multimeric glycoprotein synthesized by megakaryocytes and endothelial cells and stored in platelet α -granules and WPBs, respectively. Upon hemostatic challenge, VWF can be released from endothelial WPBs to tether circulating platelets to activated endothelial cells⁵ or exposed collagen on the vessel wall⁶. Anchoring of VWF to endothelial cells has been shown to be mediated by P-selectin⁷ and integrin $\alpha_v\beta_3$ ⁸. The subsequent release of platelet α -granule stores can further increase localized VWF concentrations to stabilize platelet-platelet interactions for platelet plug formation, the scaffold needed for the propagation of the coagulation cascade and fibrin deposition. The platelet-binding activity of VWF is regulated by its multimeric structure, with high-molecular weight multimers possessing greater hemostatic activity^{9,10}. In circulation, VWF also acts as a carrier for the coagulation factor VIII.

Fluid shear stress is an essential regulator of VWF physiology. In the absence of shear stress, VWF exists in a globular form, concealing binding domains for platelet glycoprotein Ib adhesion¹¹. When shear stress is present, the cleavage site for a metalloprotease, ADAMTS13, is exposed. ADAMTS13 cleaves naked and platelet-decorated VWF strings to regulate multimer size, thereby reducing its hemostatic activity¹².

VWF is an acute-phase protein, and numerous stimuli, including hypoxia¹³, infection¹⁴, and proinflammatory cytokines, have been shown to mediate VWF release from endothelial cells. Similar to other inflammatory agents, extracellular histones have also been shown to induce systemic VWF release in mice^{15,16} and the activation of platelets *in vitro*^{17,18,19}. This was shown to be dependent upon histone subtype, as differences in lysine and arginine content may influence function¹⁵. Our study aims to establish a flow chamber model to investigate the influence of lysine-rich (HK) and arginine-rich (HR) histone subtypes and secretagogues on endothelial VWF release and real-time platelet capture, potential early events in inflammation-induced thrombosis.

This flow chamber methodology recapitulates *in vivo* interactions between subendothelial collagen, endothelial cells, VWF, and platelets in an *in vitro* system that is visual, reproducible, and quantifiable. It allows for the real-time assessment of all aspects of the pathway that regulates VWF-platelet interactions, including WPB secretion, platelet activation, and VWF proteolysis. Studies of VWF under controlled shear stress conditions have been used to evaluate VWD mutations that impair VWF release and platelet-binding function²⁰, WPB physiology²¹, and VWF cleavage by ADAMTS13⁵. We use this methodology to quantify VWF-platelet string formation as a consequence of an inflammatory stimulus: extracellular histones.

Protocol

These studies were approved by the Research Ethics Board of Queen's University, Canada.

1. Endothelial Cell Stimulation

- Collagen-coat a 6-well tissue culture plate.**
 - 24 h in advance, coat a 6-well tissue culture plate at 37 °C with 1 mL of collagen buffer (50 µg/mL rat tail collagen type 1 with 0.02 M glacial acetic acid).
 - Wash the wells twice with 2 mL of Hank's Balanced Salt Solution (HBSS).
NOTE: Plates can be wrapped in tin foil and stored in an airtight plastic bag at 4 °C.
- Seed the endothelial cells at a density of 1×10^6 cells per well in 2 mL of growth medium containing 10% fetal bovine serum (FBS). Incubate the cells for 24 h at 37 °C (5% CO₂).
NOTE: Here, blood outgrowth endothelial cells (BOECs) between passages 5 and 15 were used. BOECs were isolated from healthy volunteers with a wildtype VWF sequence using a method referenced in Starke *et al.*²² in a manner similar to one previously described by JoVE²³.
- Remove the medium after 24 h and wash the cells with HBSS.
- Add 1 mL of serum-free medium (minimal essential growth medium without FBS) containing phorbol 12-myristate 13-acetate (PMA; 100 nM), unfractionated histone (UH), and HK or HR (all at 25 µg/mL) to the cells for 2 h at 37 °C (5% CO₂).
NOTE: This concentration of histone was based on previous *in vitro* cytotoxicity reports by Xu *et al.*²⁴ and Abrams *et al.*²⁵ that used 50 µg/mL.
- Collect the medium after 2 h and store it at -20 °C until analysis.

2. VWF Quantification by Enzyme-linked Immunosorbent Assay (ELISA)

- Coat a microplate with 100 µL of coating buffer (10 mM dibasic sodium phosphate and 145 mM sodium chloride, pH 7.2) containing 10 µg/mL polyclonal anti-VWF antibody overnight at 4 °C.
- Wash the plate three times with 250 µL of wash buffer (10 mM dibasic sodium phosphate, 500 mM sodium chloride, and 0.1% Tween 20, pH 7.2).
- Dilute the medium samples 1:2 and 1:4 with wash buffer and use normal reference plasma for a standard curve, beginning at a 1:10 dilution.
- Plate 100 µL of diluted samples and standards overnight at 4 °C.
- Wash the plate three times with 250 µL of wash buffer.
- Add 100 µL of diluted anti-VWF, HRP-conjugated detection antibody (1.1 µg/µL in wash buffer) to the plate and incubate for 1 h at room temperature.
- Wash the plate and incubate for 10 min with O-Phenylenediamine dihydrochloride (OPD) reagent, as per the manufacturer's instructions.
- Stop the reaction with 100 µL of 1 M H₂SO₄ and read the plate at 492 nm.

3. Solid-phase Histone-VWF Binding Assay

- Coat a microplate with histones diluted in 0.5% sodium deoxycholate 50 mM carbonate buffer (pH 9.6) to 10 µg/mL overnight at 4 °C.
- Wash the plate three times with 250 µL of PBS supplemented with 0.1% Tween 20, incubating for 10 min between washes.
- Block the plate with 200 µL of PBS supplemented with 0.1% Tween 20 and 1% bovine serum albumin (BSA) for 1 h at room temperature.
- Repeat step 3.2.
- Serially dilute plasma-derived human VWF/factor VIII complex from 200 mU/mL to 25 mU/mL in saline buffer (10 mM dibasic sodium phosphate, 500 mM sodium chloride, and 0.1% Tween 20, pH 7.2). Add 100 µL to the plate for 2 h at room temperature.
- Repeat step 3.2.
- Detect the binding of VWF to immobilized histone using 100 µL of a solution containing PBS-0.1% Tween 20 and 1:1,000 rabbit polyclonal anti-VWF antibody conjugated to HRP for 1 h at room temperature.
- Repeat step 3.2.
- Incubate the plate for 30 min with 100 µL of OPD reagent and stop the reaction with 100 µL of 1 M H₂SO₄. Measure the optical density at 492 nm.

4. Seeding Endothelial Cells onto Flow Chambers

- Load 0.5 mL of collagen-coating buffer (described in step 2.1) into a Luer-lock 1-mL syringe.
- Twist the Luer-lock end of the syringe onto the reservoir of a flow chamber slide.
- Press the plunger slowly until the entire lane is coated and each reservoir is full. Repeat for each lane and incubate the chamber at 37 °C for 24 h.
- Aspirate the collagen-coating buffer with a 200 µL pipette. Load another syringe with 1 mL HBSS and press the plunger slowly to wash each lane of the flow chamber. Aspirate the wash with a 200 µL pipette at the opposing end of the flow chamber. Repeat twice.

5. Pipette approximately 100 μL of a 3×10^6 cells/mL endothelial cell (BOEC) solution in growth medium with 10% FBS into the lane of a flow chamber.
NOTE: The seeding density of endothelial cells exceeds the capacity of the chamber. This is to ensure maximal channel coverage; non-adherent cells are removed in the subsequent wash step.
6. Incubate the chamber at 37 °C for 24 h. Change the medium every 8-12 h using Luer-lock syringes (as in step 4.4). Ensure that there are no visible bubbles in the lanes.

5. Isolating Platelets from Human Whole Blood

1. In a biological safety cabinet with a 30 G needle, add 300 μL of acid-citrate dextrose buffer (85 mM trisodium citrate, 111 mM D-glucose, and 71 mM citric acid, pH 4.5) to an additive-free 3 mL blood collection vacutainer.
2. Collect whole blood from healthy volunteers (free from anti-platelet and non-steroidal anti-inflammatory drugs for seven days) by venipuncture (three tubes of 3 mL each), following a protocol similar to that published by Bernardo *et al*²⁶.
3. Discard the first tube, as the initial tissue damage associated with the venipuncture can cause spontaneous platelet activation.
4. Gently invert the vacutainers three times to mix the blood with anticoagulant.
5. Centrifuge the vacutainers at 150 x g for 15 min at 24 °C (room temperature).
6. Slowly remove the platelet-rich plasma (supernatant) with a pipette in a biological safety cabinet and carefully transfer it to a 15-mL conical tube. Transfer the platelet-rich volume of each vacutainer to a single conical tube to avoid potential cross-activation.
NOTE: Platelet isolation should be performed in a biological safety cabinet to prevent bacterial contamination and potential artificial platelet and/or endothelial activation.
7. Centrifuge the conical tubes at 900 x g for 10 min at 24 °C (room temperature) to pellet the platelets.
8. Pipette and discard the platelet-poor supernatant.
9. Wash the pellet carefully with 1 mL of citrate-glucose-sodium (CGS) buffer (13 mM sodium citrate, 30 mM D-glucose, and 120 mM sodium chloride, pH 7.0).
NOTE: The platelets will appear in wisp-like formations when the CGS buffer is added and the pellet is gently resuspended. In samples contaminated by platelet activation, the platelets will not easily resuspend and will appear clumpy.
10. Once fully resuspended, centrifuge the samples at 900 x g for 10 min at 24 °C (room temperature).
11. Remove the CGS wash buffer and resuspend the pellet in 3 mL of Tyrode's buffer (138 mM sodium chloride, 5.5 mM D-glucose, 12 mM sodium bicarbonate, 2.9 mM potassium chloride, and 0.36 mM dibasic sodium phosphate, pH 7.4). Ensure complete resuspension of the platelets and, if aggregations are observed, discard the sample.
12. Add 1.5 μL from a 20 mM DiOC6 stock solution (dissolve 57.25 mg in 5 mL of methanol) to each 3 mL conical tube of washed platelets for a final concentration of 1 μM .
NOTE: DiOC6 is a green fluorescent mitochondrial dye used in this experiment to label platelets.
13. Aliquot 1 mL of the washed platelet solution to three 1.5-mL microcentrifuge tubes.
NOTE: The platelet volume required for this experiment is calculated based on the size of the flow chamber, the desired shear stress, and the length of the experiment (step 6.5). This protocol can be adjusted as conditions change to ensure that there is enough volume for fluid flow.
14. Use the washed platelets within 2 h of isolation.

6. Flow Apparatus Assembly

1. Attach a 70 cm piece of sterile silicone tubing (interior diameter of 1.6 mm) to a male elbow Luer connector at one end and a female Luer lock adaptor at the other.
2. Connect the female Luer lock adaptor attached to the tubing to a 20 mL syringe.
3. Repeat steps 6.1 and 6.2 twice to generate three identical syringe-tubing connections.
4. **Use a syringe pump to generate fluid flow. Input the following settings into the syringe pump: interior diameter of the syringe and flow rate.**
NOTE: A 20-mL syringe has an interior diameter of 19.55 mm. The flow rate is calculated based on the desired shear rate/shear stress and the dimensions of the flow chamber. For the flow chamber used in the current study, to achieve 1 dyn/cm^2 (observed in low venous shear), a flow rate of 9.37 $\mu\text{L}/\text{min}$ is required. Because of evidence linking histones to venous thrombosis, a moderate venous shear of 4.45 dyn/cm^2 is selected. This is also based on the assumption that the buffer has a similar viscosity to water. The flow rate is then equal to 41.7 $\mu\text{L}/\text{min}$. Equations used to calculate the flow rate for various flow chamber dimensions can be found at:
1. Set the pump to withdraw fluid using the button option on the syringe pump.
5. Load the three syringes attached to tubing on the syringe pump and tightly secure brackets around the syringes and plungers.
6. Attach a male elbow Luer to both ends of a second 20 cm piece of sterile silicone tubing.
7. Connect one elbow Luer to a blunted 18-gauge needle.
8. Repeat twice, creating three identical intake systems for the three lanes of the flow chamber.
NOTE: The silicon tubing and Luers can be washed with 10% bleach followed by distilled water before reuse. It is not recommended to reuse the flow chambers.

7. Microscope Settings

1. Use a spinning disk microscope equipped with a fully automated stage. Perform illumination with a laser launch that provides 405, 458, 491, 543, and 633 nm laser lines. Capture all images with a 20X objective. Adjust all parameters with the analysis software (http://www.well.ox.ac.uk/_asset/file/metamorph-basic-commands.pdf).
2. Select the channel settings (emission filter: 520/35), with excitation at 491 nm, for acquisition. Set the electron multiplying charge-coupled device to an electron-multiplying gain of 150, with an exposure time of 200 ms, to obtain the full dynamic data range.
NOTE: Platelets are labelled with a green fluorescent dye, DiOC6, with wavelength maxima (excitation, 482 nm; emission, 504 nm).

3. Adjust the 491 nm laser power to 20%.
4. Mark the centre of all three lanes and select 1 μm for z range and 0.5 μm for step size. Select the number of time points (*i.e.*, duration) and the time between images (*i.e.*, interval) to capture an image every 10 s; select "60 time points" per slide. Set the microscope to capture images from the three lanes and save them to a designated experiment folder.
NOTE: Because the flow chamber has three lanes, the microscope will need to toggle between three positions to capture the images.

8. VWF-platelet String Formation

1. Remove the culture medium from the flow chamber (from step 4) using the same technique as in step 4.4.
2. Add 100 μL of either histamine (25 μM), PMA (100 nM), UH, HK, or HR (all at 25 $\mu\text{g}/\text{mL}$) diluted in serum-free medium (as in step 1.4) to stimulate the BOEC monolayer for 15 min at room temperature and ambient O_2/CO_2 .
NOTE: Although not necessary for VWF release, performing this stimulation at 37 $^\circ\text{C}$ will improve VWF exocytosis²⁷.
3. Ensure that one of the three separate lanes of the flow chamber remain untreated as an experimental control.
4. Remove the medium using a 1 mL syringe and replace it with 100 - 200 μL of PBS to wash the secretagogues off of the endothelial monolayer.
5. Mount the flow chamber onto a slide stand using vascular clips to secure the chamber in place.
6. Attach the available male Luer connector on the end of the 70 cm tubing (connected to the syringe) to the reservoir of the flow chamber. Repeat for the two other flow chamber lanes.
7. Start the syringe pump to remove the PBS wash. Pipette additional PBS into the opposing flow chamber reservoir to ensure that the lanes do not run dry.
8. Observe the flow system for equivalent flow across all three lanes and then pause the syringe pump.
9. Select an area to capture the images in about the middle of each lane, in roughly the same area between experiments.
NOTE: The person operating the microscope can be blinded to the experimental conditions. This step ensures that the microscope is focused prior to platelet flow (refer to step 7).
10. Attach a female luer coupler to a 5 mL syringe and then to the free male luer connector (step 6.8) and submerge the blunted needle in the 1.5 mL microcentrifuge tube containing the washed platelet solution (step 5.13). Slowly draw the platelet solution through the tubing to ensure no air bubbles within the system.
11. Remove the 5 mL syringe and attach the male Luer to the open reservoir of the flow chamber. Repeat for the three lanes.
12. Restart the syringe pump and capture images during platelet flow using the microscope and protocol settings from step 7 for 10 min in the dark.
13. After 10 min, disconnect the Luer from the intake tubing on the flow chamber reservoir and fill the reservoir with PBS to maintain flow over the endothelial monolayer.

9. VWF-platelet String Quantification

NOTE: The continuous flow of PBS is required to maintain the VWF-platelet string elongation for image analysis. Cessation of flow will result in the VWF becoming globular and will impair VWF-platelet string quantification. It is essential to top up each reservoir with PBS during image capture. HBSS can replace PBS if cell shrinking or detachment is observed during this step.

1. Beginning with the first lane, capture 10 images per slide without overlap using a 20X objective lens around middle of the slide. Repeat this for each lane.
NOTE: The areas surrounding the reservoirs should be avoided due to turbulent shear stress.
2. Using image processing software, adjust the brightness by clicking "Image," "Adjust," and "Brightness/Contrast." Drag the scroll bar until the adhered platelets can be viewed well enough for quantification.
3. Record a VWF-platelet string when three or more aligned platelets are observed in the image. Count all the VWF-platelet strings in an image. Repeat for all 10 images and average for the experiment.
NOTE: The person performing the quantification can be blinded to the experimental conditions. It is not necessary to co-stain for VWF, as this has been confirmed by independent studies^{8,28,29}.
4. Repeat the experiment a minimum of three times to evaluate each secretagogue.

Representative Results

To directly assess the effect of histones on VWF release from endothelial cells, we exposed confluent BOECs to serum-free medium containing PMA (positive control), UH, HR, and HK for 2 h. We showed that HK induced a 2-fold increase in VWF protein (VWF:Ag) in the medium of treated endothelial cells (**Figure 1**). Interestingly, when BOECs were stimulated with UH and HR, there was less VWF:Ag detected in the medium than in the untreated condition. We hypothesized that because histones can bind directly to VWF³⁰, they may differentially interfere with VWF:Ag detection in the culture medium. To evaluate histone binding to VWF, we used a solid-phase binding assay. We showed that UH and HR bound more strongly to VWF than HK (**Figure 2**), supporting the detection interference demonstrated in **Figure 1**.

Extracellular histones have been shown to activate platelets *in vitro*¹⁹, and our data suggest that histones mediate VWF release from endothelial cells. To characterize the effect of histones on VWF-platelet interactions, we used a flow chamber model of VWF-platelet string formation in which labelled platelets were perfused on stimulated endothelial cells. Representative images were captured post-flow, and the number of VWF-platelet strings were quantified.

We observed that, following the initiation of flow conditions, untreated cells had very few VWF-platelet strings (<1 string per review field), while histamine and PMA-treated cells had an average of 2.10 and 3.10 strings, respectively. Significantly more VWF-platelet strings were formed when cells were treated with HK (3.52 strings, $P = 0.019$), HR (6.00 strings, $P = 0.004$), and UH (5.51 strings, $P = 0.012$). A graphical representation of the VWF-platelet string count is shown in **Figure 3G**. Real-time VWF-platelet string formation in response to UH compared to untreated cells is shown in **Videos 1A and B**.

These studies, along with investigations by other groups, show that histones²⁸ and other proinflammatory agents such as histamine⁵ and cytokines³¹ stimulate VWF secretion from endothelial cells, mediating subsequent platelet capture *in vitro*. We demonstrated that the static stimulation of endothelial cells was not sufficient to elucidate VWF release due to the capability of histones to bind and sequester VWF. The design of a flow chamber model of VWF release and platelet adhesion was therefore required to more completely characterize and model the *in vivo* interactions between the endothelium, VWF, and platelets.

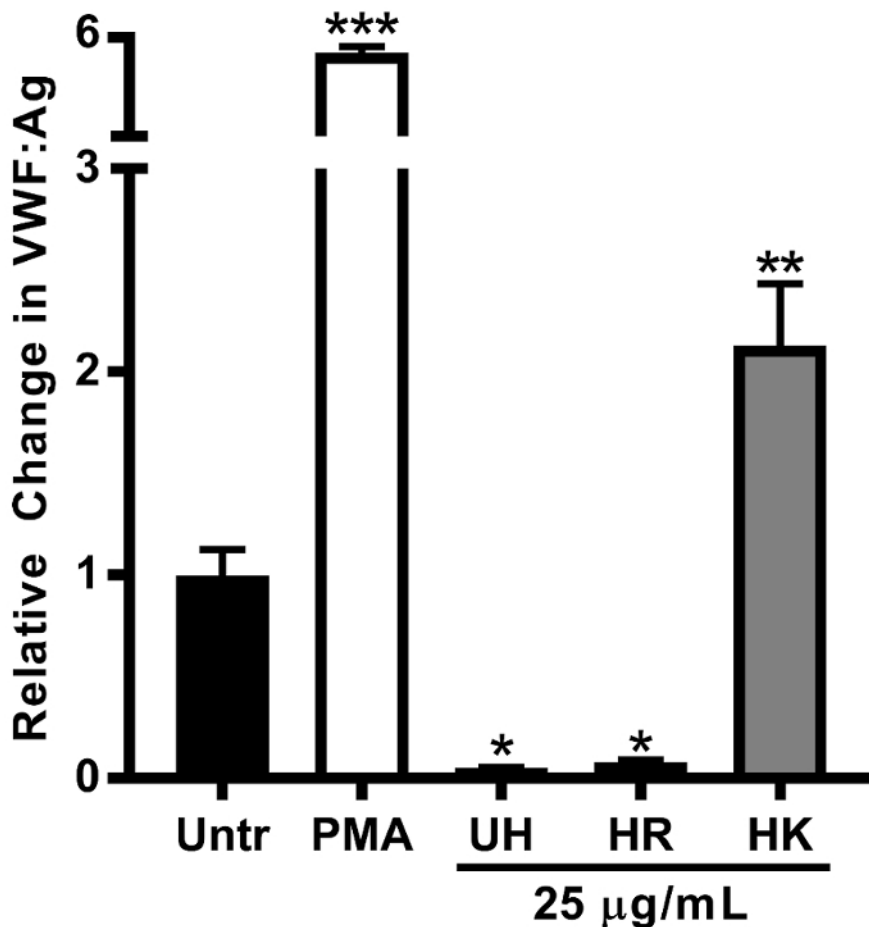


Figure 1: Lysine-rich Histones Induces VWF Release from Cultured Endothelial Cells. BOECs were stimulated with unfractionated histone (UH), lysine-rich (HK), and arginine-rich (HR) histone fractions. HK stimulated VWF release into the culture medium. UH and HR treatment decreased the detection of VWF:Ag in the endothelial cell medium relative to the untreated (Untr) control. $N \geq 3$ individual experiments were performed. The data are shown as the mean values \pm SE. * $P < 0.05$, ** $P < 0.01$, and *** $P < 0.001$ indicate the significance relative to the untreated condition. This figure has been modified from Michels *et al*¹⁵. [Please click here to view a larger version of this figure.](#)

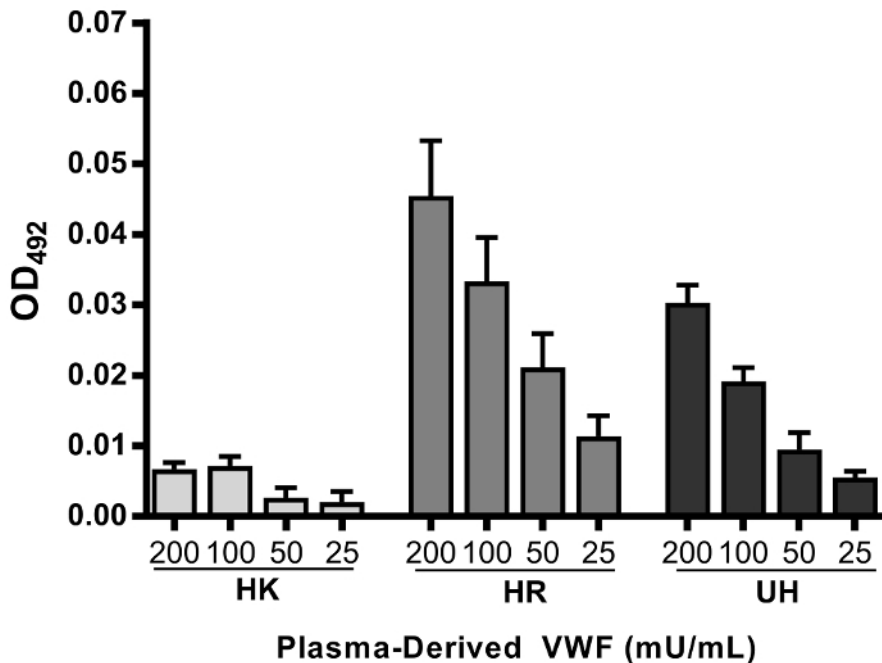


Figure 2: VWF-histone Binding Interferes with VWF Detection *In Vitro*. Plasma-derived VWF binds more strongly to HR and UH in a dose-dependent fashion compared to lysine-rich (HK) histones in a solid-phase binding assay. The data are shown as the mean values \pm SE. $N \geq 3$ individual experiments were performed. This figure has been modified from Michels *et al*¹⁵. [Please click here to view a larger version of this figure.](#)

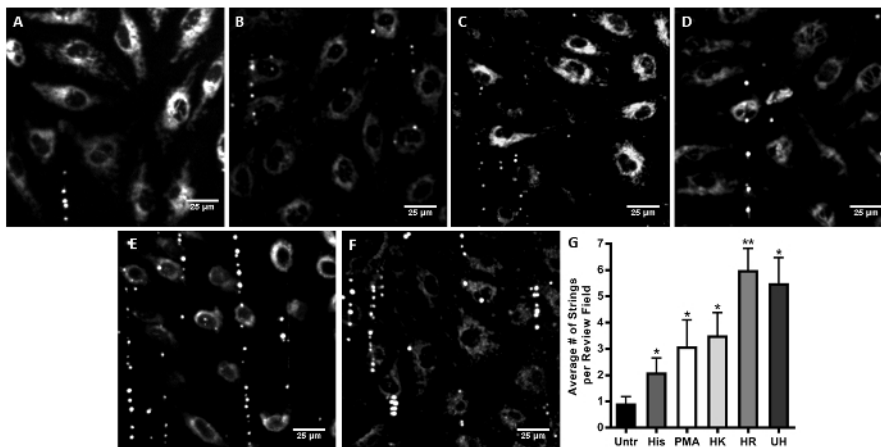


Figure 3: Histones Mediate VWF-platelet String Formation. Endothelial cells seeded on flow chamber slides were treated with unfractionated histone (UH), lysine-rich (HK), or arginine-rich (HR) histone fractions or histamine/PMA (positive controls) and were perfused at a shear stress of 4.45 dyn/cm² for 10 min with washed, fluorescently labeled platelets. Representative images were obtained post-platelet flow from the untreated control (A) and cells treated with histamine (B), Phorbol 12-myristate 13-acetate (PMA) (C), HK (D), HR (E), and UH (F). PMA treatment resulted in an average of 3.1 strings per field of view, comparable to histamine. VWF-platelet strings were quantified from 10 consecutive review fields and averaged for $n \geq 3$ individual experiments (G). The data are shown as the mean values \pm SE. * $P < 0.05$ and ** $P < 0.01$ indicate significance relative to the untreated condition. This figure has been modified from Michels *et al*¹⁵. [Please click here to view a larger version of this figure.](#)

Supplemental Videos. VWF-platelet String Formation in Response to Unfractionated Histone (2) Compared to No Treatment (1): This video has been modified from Michels *et al*¹⁵. [Please click here to download these videos.](#)

Discussion

While the physiological relevance of VWF-platelet strings remains controversial due to their rapid dissolution in the presence of the VWF-cleaving protease ADAMTS13, they serve as a quantifiable *in vitro* model of platelet recruitment by VWF to a site at which a thrombus might form in the presence of localized increases in histone levels⁵. Moreover, in pathologies lacking ADAMTS13 activity-such as thrombotic thrombocytopenic purpura (TTP)-or in inflammatory microenvironments-where ADAMTS13 activity is inhibited-VWF-platelet strings can be observed *in vivo*³² and may contribute to platelet microaggregation and leukocyte extravasation, linking the hemostatic and proinflammatory

functions of VWF³³. Finally, it has been hypothesized that VWF-platelet string formation might be an initiating event in venous and/or arterial thrombosis, forming the nidus around which a pathological thrombus is built.

VWF-platelet string formation in the flow chamber system can be used to study WPB exocytosis, ADAMTS13 cleavage, and the platelet binding capacity of VWF. There are several critical steps to successfully executing these experiments. However, depending on the application of the model, modifications can be made to the protocol.

Endothelial cells from specific vascular beds are heterogeneous in their response to mechanical and biochemical signals³⁴. It may therefore be useful to select a cell type suitable for the application of this methodology. BOECs were used in the current study because of their proliferative potential; maintenance of phenotype across several (10+) passages; and robust VWF expression, facilitating the quantification of VWF exocytosis. Other investigators have used human umbilical vein endothelial cells (HUVECs)^{5,8,28} and non-endothelial cells (human embryonic kidney 293 cells) transfected with VWF cDNAs expressing VWD mutations³⁵. It has been demonstrated that VWF expression varies significantly between tissue and vessel physiology³⁶. Cultured endothelial cells arising from various micro- and macrovasculature have observable differences in VWF protein basal secretion³⁷, and there is evidence that calcium channel differences between endothelial cell subtypes influence WPB exocytosis in response to secretagogues³⁸.

Histones were used in this study as a novel secretagogue. They were compared to the positive control, histamine, a frequently described physiological stimulant of VWF release. A VWF:Ag ELISA was used to verify VWF release from endothelial cells under static conditions. There are two intracellular mechanisms that trigger the release of VWF: the elevation of intracellular calcium³⁹ or pf cyclic AMP levels⁴⁰. Differential activation of these pathways can be induced by secretagogues such as thrombin/histamine or epinephrine/vasopressin (or, relevant to VWD, desmopressin), respectively, and it may be interesting to compare these two pathways using this flow chamber model of VWF-platelet string formation. In the context of thrombo-inflammatory disease, further elucidation of inflammatory biomarkers, such as cytokines⁴¹ or damage/pathogen-associated molecular patterns (DAMPs/PAMPs), and their roles in VWF-platelet string formation is encouraged.

Fluid shear stress is important when globular VWF unfolds to expose the A1 domain binding site for glycoprotein Ib on platelets¹¹. It has been demonstrated that a minimum fluid shear stress of approximately 0.73 dyn/cm² is required for platelet binding to VWF strings⁴². Furthermore, these strings form on endothelial cells at relatively low shear stresses (2.5 dyn/cm²) but can be dislodged at shear stresses of 20 dyn/cm² or above⁸. In the current investigation, we selected a venous shear stress (4.45 dyn/cm²) that allowed for interactions between the endothelium, VWF, and platelets while conserving the perfusion buffer for a 10 min experiment.

Using this flow chamber system to evaluate ADAMTS13 cleavage of VWF-platelet strings requires an increase in the fluidic shear stresses over those used in this experiment. Maximal ADAMTS13 cleavage of VWF-platelet strings occurs between 10 and 30 dyn/cm²¹², a range that encompasses high venous to moderate arterial shear stress⁴³. Modifying the shear rate in this system may be useful for comparing VWF-platelet string formation and dissolution, contributing factors in the development of venous, arterial, or microvascular thrombosis.

Additional modifications of this technique can be made to the perfusion material and the flow chamber. Secretagogues can be administered under flow conditions to resemble *in vivo* environments. Priming platelets with agonists to evaluate their reactivity or including leukocyte populations are extensions of this technique. Furthermore, including therapeutic agents targeting VWF multimer length, platelet binding capacity, or platelet reactivity may elucidate important mechanisms that regulate the initiation of thrombus development. Other investigators have used either in-house⁴⁴ or purchased glass coverslip flow chambers⁴⁵, as opposed to the polymer-based slides used in this study, and seem to obtain comparable results.

A critical consideration in the VWF-platelet string protocol is the preparation of washed platelets. It is not recommended to use whole blood in this protocol due to the presence of ADAMTS13. Agents preventing platelet activation, such as prostacyclin or apyrase, should be avoided, as this may later adversely influence platelet adhesion to VWF. Ensuring that the buffers are brought to room temperature prior to platelet isolation and using careful pipette techniques (*i.e.*, avoiding bubbles and harsh shear stresses) are key to maintaining the platelets in their inactive state. Furthermore, labeling platelets with a mitochondrial stain, such as DIOC6 or rhodamine 6G, is preferred over interfering with extracellular domains that may be important for VWF binding. However, as DIOC6 is a membrane-permeable dye, it may also be taken up in small quantities by the endothelial cells over the course of the experiment. In the absence of a fluorescent microscope, other studies have observed VWF-platelet strings using bright-field microscopy⁴⁶.

In conclusion, this flow chamber methodology of VWF-platelet string formation can provide mechanistic, real-time data to support *in vivo* observations in the pathogenesis of thrombosis. As exposure to shear strongly influences the pathophysiological role that VWF plays in thrombo-inflammatory disease, the flow chamber model is a vital investigative tool for any lab interested in understanding endothelial cell-platelet interactions in this context.

Disclosures

The authors declare no competing financial interests.

Acknowledgements

Alison Michels is a recipient of a Frederick Banting and Charles Best Canada Graduate Scholarship from the Canadian Institutes of Health Research (CIHR). Laura L. Swystun is the recipient a CIHR fellowship. David Lillcrap is the recipient of a Canada Research Chair in Molecular Hemostasis. This study was funded in part by a CIHR operating grant (MOP-97849).

References

1. Roger, V. L. *et al.* Heart disease and stroke statistics--2011 update: a report from the American Heart Association. *Circulation*. **123** (4), e18-e209 (2011).
2. Sadler, J. E. von Willebrand factor: two sides of a coin. *J Thromb Haemost*. **3** (8), 1702-1709 (2005).
3. Koster, T., Blann, A. D., Briët, E., Vandenbroucke, J. P., Rosendaal, F. R. Role of clotting factor VIII in effect of von Willebrand factor on occurrence of deep-vein thrombosis. *Lancet*. **345** (8943), 152-5 (1995).
4. Morange, P. E. *et al.* Endothelial Cell Markers and the Risk of Coronary Heart Disease: The Prospective Epidemiological Study of Myocardial Infarction (PRIME) Study. *Circulation*. **109** (11), 1343-1348 (2004).
5. Dong, J. F. *et al.* ADAMTS-13 rapidly cleaves newly secreted ultralarge von Willebrand factor multimers on the endothelial surface under flowing conditions. *Blood*. **100** (12), 4033-4039 (2002).
6. Ruggeri, Z. M. Von Willebrand factor, platelets and endothelial cell interactions. *J Thromb Haemost*. **1** (7), 1335-1342 (2003).
7. Padilla, A. *et al.* P-Selectin anchors newly released ultralarge von Willebrand factor multimers to the endothelial cell surface P-selectin anchors newly released ultralarge von Willebrand factor multimers to the endothelial cell surface. *Blood*. **103** (6), 2150-2156 (2004).
8. Huang, J., Roth, R., Heuser, J. E., Sadler, J. E. Integrin α v β 3 on human endothelial cells binds von Willebrand factor strings under fluid shear stress. *Blood*. **113** (7), 1589-1598 (2009).
9. Moake, J. L., Turner, N. A., Stathopoulos, N. A., Nolasco, L. H., Hellums, J. D. Involvement of large plasma von Willebrand Factor (vWF) multimers and unusually large vWF forms derived from endothelial cells in shear stress-induced platelet aggregation. *J Clin Invest*. **78** (6), 1456-1461 (1986).
10. Federici, A. B., Bader, R., Pagani, S., Colibretti, M. L., De Marco, L., Mannucci, P. M. Binding of von Willebrand factor to glycoproteins Ib and IIb/IIIa complex: affinity is related to multimeric size. *Br J Haematol*. **73**, 93-99 (1989).
11. Goto, S., Salomon, D. R., Ikeda, Y., Ruggeri, Z. M. Characterization of the Unique Mechanism Mediating the Shear-dependent Binding of Soluble von Willebrand Factor to Platelets Characterization of the Unique Mechanism Mediating the Shear-dependent Binding of Soluble von Willebrand Factor to Platelets. *J Biol Chem*. **270** (40), 23352-23361 (1995).
12. Shim, K., Anderson, P. J., Tuley, E. A., Wiswall, E., Sadler, J. E. Platelet-VWF complexes are preferred substrates of ADAMTS13 under fluid shear stress. *Blood*. **111** (2), 651-657 (2008).
13. Pinsky, D. J. *et al.* Hypoxia-induced exocytosis of endothelial cell Weibel-Palade bodies: A mechanism for rapid neutrophil recruitment after cardiac preservation. *J Clin Invest*. **97** (2), 493-500 (1996).
14. Luttge, M. *et al.* Streptococcus pneumoniae induces exocytosis of Weibel-Palade bodies in pulmonary endothelial cells. *Cell Microbiol*. **14** (2), 210-225 (2012).
15. Michels, A. *et al.* Histones link inflammation and thrombosis through the induction of Weibel - Palade body exocytosis. *J Thromb Haemost*. **14** (11), 2274-2286 (2016).
16. Brill, A. *et al.* Neutrophil extracellular traps promote deep vein thrombosis in mice. *J Thromb Haemost*. **10** (1), 136-144 (2012).
17. Semeraro, F. *et al.* Extracellular histones promote thrombin generation through platelet-dependent mechanisms: involvement of platelet TLR2 and TLR4. *Blood*. **118** (7), 1952-1961 (2011).
18. Ammolle, C. T., Semeraro, F., Xu, J., Esmon, N. L., Esmon, C. T. Extracellular histones increase plasma thrombin generation by impairing thrombomodulin-dependent protein C activation. *J Thromb Haemost*. **9** (9), 1795-1803 (2011).
19. Carestia, A., Rivadeneyra, L., Romaniuk, M. A., Fondevila, C., Negroto, S., Schattner, M. Functional responses and molecular mechanisms involved in histone-mediated platelet activation. *Thromb Haemost*. **110** (5), 1035-1045 (2013).
20. Wang, J. W. *et al.* Analysis of the storage and secretion of von Willebrand factor in blood outgrowth endothelial cells derived from patients with von Willebrand disease. *Blood*. **121** (14), 2762-2772 (2013).
21. Ferraro, F. *et al.* Weibel-Palade body size modulates the adhesive activity of its von Willebrand Factor cargo in cultured endothelial cells. *Sci Rep*. **6** (August), 32473 (2016).
22. Starke, R. D. *et al.* Cellular and molecular basis of von Willebrand disease: studies on blood outgrowth endothelial cells. *Blood*. **121** (14), 2773-2784 (2013).
23. Ormiston, M. L. *et al.* Generation and Culture of Blood Outgrowth Endothelial Cells from Human Peripheral Blood. *J Vis Exp*. **106**, e53384 (2015).
24. Xu, J. *et al.* Extracellular histones are major mediators of death in sepsis. *Nat Med*. **15** (11), 1318-1321 (2009).
25. Abrams, S. T. *et al.* Circulating histones are mediators of trauma-associated lung injury. *Am J Respir Crit Care Med*. **187** (2), 160-169 (2013).
26. Bernardo, A., Ball, C., Nolasco, L., Choi, H., Moake, J. L., Dong, J. F. Platelets adhered to endothelial cell-bound ultra-large von Willebrand factor strings support leukocyte tethering and rolling under high shear stress. *J Thromb Haemost*. **3** (3), 562-570 (2005).
27. Hewlett, L. *et al.* Temperature-dependence of weibel-palade body exocytosis and cell surface dispersal of von willebrand factor and its polypeptide. *PLoS ONE*. **6** (11) (2011).
28. Lam, F. W., Cruz, M. A., Parikh, K., Rumbaut, R. E. Histones stimulate von Willebrand factor release in vitro and in vivo. *Haematologica*. **101** (7), e277-e279 (2016).
29. Zheng, Y., Chen, J., López, J. A. Flow-driven assembly of VWF fibres and webs in in vitro microvessels. *Nat Commun*. **6** (7858) (2015).
30. Ward, C. M., Tetaz, T. J., Andrews, R. K., Berndt, M. C. Binding of the von Willebrand factor A1 domain to histone. *Thromb Res*. **86** (6), 469-477 (1997).
31. Bernardo, A., Ball, C., Nolasco, L., Moake, J. F., Dong, J. F. Effects of inflammatory cytokines on the release and cleavage of the endothelial cell-derived ultralarge von Willebrand-factor multimers under flow. *Blood*. **104** (1), 100-106 (2004).
32. De Ceunynck, K., De Meyer, S. F., Vanhoorelbeke, K. Unwinding the von Willebrand factor strings puzzle. *Blood*. **121** (2), 270-277 (2013).
33. Petri, B. *et al.* von Willebrand factor promotes leukocyte extravasation. *Blood*. **116** (22), 4712-4719 (2010).
34. Aird, W. C. Endothelial cell heterogeneity. *Cold Spring Harb Perspect Med*. **2** (1), 1-13 (2012).
35. Wang, J. W. *et al.* Formation of platelet-binding von Willebrand factor strings on non-endothelial cells. *J Thromb Haemost*. **10** (10), 2168-2178 (2012).
36. Yamamoto, K., de Waard, V., Fearn, C., Loskutoff, D. J. Tissue Distribution and Regulation of Murine von Willebrand Factor Gene Expression In Vivo. *Blood*. **92** (8), 2791-2801 (1998).

37. Shahani, T., Lavend'homme, R., Luttun, A., Saint-Remy, J. M., Peerlinck, K., Jacquemin, M. Activation of human endothelial cells from specific vascular beds induces the release of a FVIII storage pool. *Blood*. **115** (23), 4902-4909 (2010).
38. Wu, S. *et al.* CaV3.1 ($\alpha 1G$) T-type Ca^{2+} channels mediate vaso-occlusion of sickled erythrocytes in lung microcirculation. *Circ Res*. **93** (4), 346-353 (2003).
39. Knop, M., Gerke, V. Ca^{2+} -regulated secretion of tissue-type plasminogen activator and von Willebrand factor in human endothelial cells. *Biochim Biophys Acta*. **1600** (1-2), 162-167 (2002).
40. Vischer, U., Wollheim, C. Epinephrine induces von Willebrand factor release from cultured endothelial cells: involvement of cyclic AMP-dependent signalling in exocytosis. *Thromb Haemost.* **77** (6), 1182-1188 (1997).
41. Bernardo, A., Ball, C., Nolasco, L., Moake, J. F., Dong, J. F. Effects of inflammatory cytokines on the release and cleavage of the endothelial cell-derived ultralarge von Willebrand factor multimers under flow. *Blood*. **104** (1), 100-106 (2004).
42. Kumar, R. A., Dong, J. F., Thaggard, J. A., Cruz, M. A., López, J. A., McIntire, L. V Kinetics of GPIIb/IIIa-vWF-A1 tether bond under flow: effect of GPIIb/IIIa mutations on the association and dissociation rates. *Biophys J*. **85** (6), 4099-4109 (2003).
43. Lipowsky, H. H., Usami, S., Chien, S. In vivo measurements of "apparent viscosity" and microvessel hematocrit in the mesentery of the cat. *Microvasc Res*. **19** (3), 297-319 (1980).
44. De Ceunynck, K. *et al.* Local elongation of endothelial cell-anchored von Willebrand factor strings precedes ADAMTS13 protein-mediated proteolysis. *J Biol Chem*. **286** (42), 36361-36367 (2011).
45. Coburn, L. A., Damaraju, V. S., Dozic, S., Eskin, S. G., Cruz, M. A., McIntire, L. V. GPIIb/IIIa-vWF rolling under shear stress shows differences between type 2B and 2M von Willebrand disease. *Biophys J*. **100** (2), 304-312 (2011).
46. Dong, J. F. *et al.* Magnesium maintains endothelial integrity, up-regulates proteolysis of ultra-large von Willebrand factor, and reduces platelet aggregation under flow conditions. *Thromb Haemost.* **99** (3), 586-593 (2008).